Effects of non-equilibrium polymer conformations on the adhesive strength of an interface

K. P. O'Connor* and T. C. B. McLeish
Department of Physics, University of Sheffield, Sheffield S3 7RH, UK
(Received 24 September 1991; revised 23 January 1992; accepted 18 February 1992)

We calculate, using a tube model, the enhancement of adhesive strength between a surface-attached chain and a matrix (in the glassy phase) that is polymerized *in situ*. The conformational relaxation caused by the change in the chains' local environment may or may not be dominated by entanglements. We conclude that in the favourable scenario of slow relaxation dynamics and rapid polymerization and subsequent quench (by glassification), the adhesive strength may be increased up to a factor $(a/b)^{1/3}$, where a is the tube diameter and b is the Kuhn length for the attached chain.

(Keywords: adhesives; chain entanglement; polymerization; conformations; interface; modelling)

INTRODUCTION

The adhesion of polymer interfaces is a problem of practical importance, with applications in coatings and reinforcement. This has motivated a number of experimental and theoretical studies[1–4]. Adhesion of bulk polymer to a non-polymeric surface may be improved by the chemical attachment of some chains to the surface, which gives the interface a similar character to a polymer/polymer weld. In the latter case, chain dynamics prior to glassification affect the adhesive strength significantly[5,6]; we expect the same of end-tethered chains. One method of achieving a strong interface is to attach chains to the solid surface in a solution of their own monomers, which is then polymerized around the tethered chains. In this paper, we consider the effects of polymerization kinetics on the adhesive strength of this interface type.

Our model assumes a chain terminally attached to an infinite, neutral, flat surface surrounded by a matrix of chemically identical chains. The surface coverage σ is small, $\sigma < N^{-6/5}$, such that there are no interactions between neighbouring chains; the average properties of a single chain are considered. We concentrate on adhesion in the regimes where failure of the interface is dominated by the pull-out of the attached chain from the matrix rather than chain scission.

An interface of this type is relatively simple to model as it is strictly flat, there is only one crossing per attached polymer and, with a low surface coverage, crazing[7] is unlikely.

We consider how the pull-out energy may be enhanced by polymerizing the matrix *in situ*. During polymerization the attached chain collapses from a swollen to an ideal conformation, suffering a consequent reduction in entangled path length. Depending on polymerization rate and the time at which the system is quenched by glassification, the collapse itself may or may not be dominated by entanglements. By calculating the timescale of conformation relaxation, limits can be given for the polymerization rate and quench time so as to capture the maximum amount of swollen conformation, thus enhancing interface adhesion.

Our work has two parts. First we present a model for the adhesive energy contribution of end-tethered chains of general conformation. This differs from previous hypotheses[8] and considers failure at both constant stress and constant interface velocity. Secondly, we calculate how the bulk polymerization affects the dynamics of the tethered chains, and which conformations result on glassification.

TUBE MODEL FOR ADHESION

Consider a polymer of N_A monomers, terminally attached to a neutral flat surface, in a network of polymers each of N_s monomers, below the glass transition temperature (*Figure 1a*). For simplicity, we assume that the persistence length coincides with the monomer length, b. Providing that $N_s > N_e$, the network polymers can be represented as a topologically constraining tube for polymer A[9], thus restricting motion on scales larger than N_e to along the tube axis. In this paper N_e refers to the entanglement number most generally; we allow for non-equilibrium, semidilute chain conformations. The tube length is given by:

$$L = (N_A/N_e)a \tag{1}$$

where a is the tube diameter. Presented here are two limiting cases of a tube model for the interface adhesion energy, in the non-inertial limit. Our model is different from that of Evans[8] as we choose not to employ the Einstein relationship below the glass transition temperature. The pull-out energy of polymer A, E_p, is defined as

* To whom correspondence should be addressed

0032-3861/92/204314-08

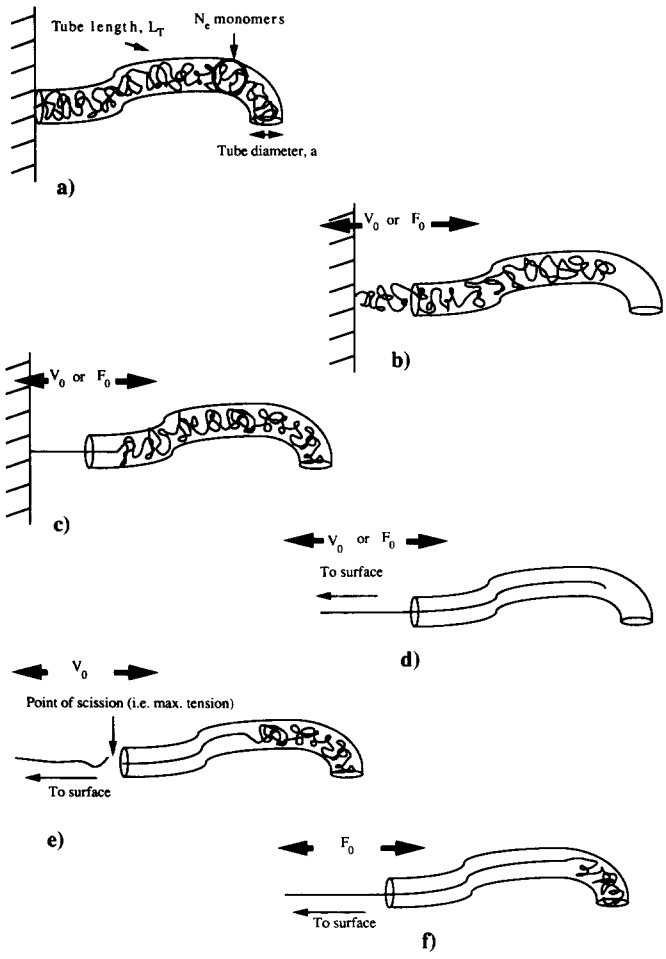

Figure 1 (a) Polymer A attached to a flat surface, inside its tube, below the glass transition temperature. The number of monomers between entanglements N_e is indicated, and is not necessarily the equilibrium value. (b) The monomers of the chain are pulled out as a whole, with either constant force or constant velocity. (c) The chain is pulled out from the tube and fully stretches from a mobilization site that proceeds down the tube. (d) If the mobilization site is able to reach the end of the tube, further pull-out occurs as in (b) but with a reduced entanglement number (a/b). (e) If in the case of constant velocity, the tension at the front of the tube exceeds F_{sc}, the chain breaks at that point. (f) If in the case of constant force, the critical force of the mobilized monomers (inside the tube) equals the applied force, the pull-out comes to a halt

the work done in pulling the polymer totally from its tube:

$$E_p = \int_0^d F(s)\,ds \tag{2}$$

$F(s)$ is the tension of the chain at the attached end, at a pull-out distance s from the 'tube mouth' such that $s=0\rightarrow d$, and d is the total length associated with the particular pull-out process. In the tube, the frictional force on a monomer is $f=\zeta v$, where v is its velocity and ζ is the monomeric friction constant. There is a minimum critical force for monomer mobilization, f_c. Equations (1) and (2) are our link between chain conformation and adhesion. Either the 'process length' d or the maximum frictional force is related to the tube length (see below), which in turn is given by the generalized entanglement number, N_e. As this is defined as the number of monomers in a chain spanning a (fixed) tube diameter a, it is a direct function of chain conformation.

For a fully stretched chain segment of N monomers, with a velocity v relative to the tube, the ratio of frictional to elastic forces is:

$$r_f \equiv \frac{\zeta v N}{3k_B T/b} \tag{3}$$

with k_B and T the Boltzmann constant and temperature respectively. If $r_f \ll 1$ then chain deformation in the pull-out process will be small. If $r_f > 1$ then the chain will totally stretch out during the pull-out process. This criterion forms the limiting cases of our model. Partial deformation is rather more complex to model and will not be dealt with here. In either case the elastic contribution to the pull-out energy will be small with respect to the frictional contribution, and thus it will be neglected. For both limits of our model we consider the conditions of:

(i) constant rate of surface/network separation, v_0;
(ii) constant force across the surface/network interface, F_0.

In all cases $v_0 = f_c/\zeta$ and $F_0 = f_c$ are respectively the absolute minimum velocity and force required for mobilization. *Table 1* shows the results for these cases and their limits for validity, using equations (1) and (2). F_{sc} denotes the tension in the chain at which scission occurs. The tube is considered to be long ($N_A \gg N_e$) so that end effects are neglected. Also the scission energy is considered to be negligible with respect to pull-out energy.

Cases A and B (*Figure 1b*) have a process length of that of the tube, L. With constant pull-out velocity, the frictional force experienced by the tube is proportional to the number of monomers residing inside it. The limits on v_0 dictate that all the chain monomers can be simultaneously mobilized and that there is only small deformation when the tension is maximum, at the start of pull-out. Similarly, the limits on F_0 allow whole chain mobilization with no deformation; however, the tension at the front of the tube is constant throughout the process.

In the cases of C and D (*Figure 1c*) the chain tension increases as more monomers are mobilized from a site moving back into the tube. Thus, there is the possibility that the chain tension may, at some point, exceed the

Table 1

Case		Pull-out energy, E_p	Limits on application	
A	No deformation, constant velocity	$\dfrac{\zeta v_0 a N_A^2}{2N_e}$	$v_0 \ll \dfrac{3kT}{b\zeta N_A}$	
B	No deformation, constant force	$\dfrac{F_0 a N_A}{N_e}$	$N_A f_c < F_0 \ll \dfrac{3kT}{b}$	
C	Full deformation, constant velocity	$\dfrac{\zeta v_0 a N_A^2}{2N_e}$		$v_0 < \dfrac{bN_e F_{sc}}{a\zeta N_A}$
D	Full deformation, constant velocity (scission)	$\left(\dfrac{bN_e}{a}-1\right)\dfrac{F_{sc}^2 b}{2\zeta v_0}$	$f_c \geqslant \dfrac{3kT}{b}$	$v_0 > \dfrac{bN_e F_{sc}}{a\zeta N_A}$
E	Full deformation, constant force	$F_0 N_A b$		$F_0 > \dfrac{f_c a N_A}{bN_e}$
F	Full deformation, constant force (halting)	$\dfrac{F_0^2 b}{f_c}$		$F_0 < \dfrac{f_c a N_A}{bN_e}$

scission tension and break (*Figure 1d*). The maximum chain tension arises when the mobilization site reaches the end of the tube. If this maximum tension is less than the scission tension, then further pull-out proceeds in a similar manner to case A except that, as the chain is fully stretched, $N_e \rightarrow (a/b)$ (*Figure 1e*). However, if the chain does undergo scission, the process length is proportional to F_{sc}.

With cases E and F, if the chain is to undergo scission, then it will do so at the start of pull-out. These cases are similar to C and D but, instead of scission occurring, if the critical friction of the mobilized monomers equals the applied force F_0, the pull-out will halt (*Figure 1f*). In this case the process length is proportional to F_0.

We include here for clarity the calculation of E_p for the two-stage pull-out process, case C:

$$E_p = \frac{\zeta v}{b}\frac{L}{(N_A b - L)}\int_0^{(N_A b - L)} s\,ds + \frac{\zeta v}{b}\int_0^{L}(L-s)\,ds$$
$$= \frac{\zeta v}{b}\left(\frac{L(N_A b - L)}{2} - \frac{L^2}{2}\right) = \frac{\zeta v N_A L}{2} \qquad (4)$$

It is worth noting the fact that cases A and C yield the same pull-out energy but only case C allows for partial pull-out before scission.

We now need to find an expression for the generalized entanglement number. Formally a^2 is the mean-square displacement between entanglements at the nth and mth monomers, between which are n–m monomers of the attached chain. At time t during an arbitrary dynamical process, $N_e(t) = |n-m|$, such that:

$$a^2 = \langle [\boldsymbol{R}_n(t) - \boldsymbol{R}_m(t)]^2 \rangle \qquad (5)$$

where $\boldsymbol{R}_n(t)$ is the vector to monomer n from an arbitrarily defined origin, and is known, at least stochastically, for any chain dynamics we consider. To find $N_e(t)$ we require the as yet undetermined function $\langle [\boldsymbol{R}_n(t) - \boldsymbol{R}_m(t)]^2 \rangle$ in the form $F(|n-m|, t)$, and then rearrange to get $N_e(t) = F^{-1}(a^2, t)$. We know a for a particular polymer at fixed density. We note here that a value of $N_e(t)$ less that its equilibrium value corresponds to a stretched polymer and an increased adhesive strength.

POLYMERIZATION

Now consider the solvent polymerization around the attached polymer, A. We use a simple, monodisperse, model of polymerization kinetics, whereby a chain grows by monomer addition:

$$N_s(t) = N_s(\infty)[1 - \exp(-t/\tau_{pol})] \qquad (6)$$

where τ_{pol} is the characteristic polymerization time. $N_s(\infty)$ can be freely chosen as $N_s(\infty) = 1/\phi$, where ϕ is the initiator concentration. During polymerization the polymer density of the solution increases, causing the swollen polymer to contract as its self-avoidance is screened[10]. At a time t_q after polymerization initiation, the system is quenched by glassification, so there is no further relaxation:

$$\langle [\boldsymbol{R}_n(t) - \boldsymbol{R}_m(t)]^2 \rangle = \text{constant} \qquad t > t_q \qquad (7)$$

The outcome of the quenched polymerization is largely dictated by the ratio:

$$r_\tau \equiv \tau_{pol}/\tau_{rel} \qquad (8)$$

where τ_{rel} is the characteristic time for the relaxation dynamics of polymer A. In the simple case for which $r_\tau \gg 1$, the conformation of the chain reaches its Gaussian equilibrium; there is no adhesion enhancement in this case. We consider first regimes for which $r_\tau \ll 1$, which is equivalent to instantaneously 'switching' the environment of polymer A from that of swollen to Gaussian statistics. Further, we present in this regime the two cases of solely entangled and unentangled dynamics. With respect to the degree of polymerization of the melt, the transition from the unentangled to the entangled regime is observed to be $N = \alpha N_e$, where $\alpha \sim 2$–7 depending on the polymer type and experimental quantities measured[11]. The apparent ambiguity in requiring the melt to be unentangled, and the glassy phase to be entangled, can be rectified by employing the concept of constraint release. By considering polymer A as a long chain in a sea of short solvent polymers, it only *effectively* becomes entangled when $N_s(\infty) > (N_A N_e^2)^{1/3}$ (ref. 12); however, constraint release is of course absent in the glassy phase. Thus the regime of solely unentangled dynamics in the melt requires the condition:

$$\alpha N_e < N_s(\infty) < (N_A N_e^2)^{1/3} \qquad (9)$$

When considering the well entangled regime, $N_s(\infty)$ has to be greater than both limits in equation (9). Finally, we consider the more realistic regime where there is no restriction on r_τ (i.e. we can choose $r_\tau \sim 1$), so we have both entangled and unentangled dynamics present *during* polymerization.

We do not present a full treatment of surface perturbed chain conformations here. We look at a chain with one end fixed in 'free solution', and later apply some results from the literature[15] to make some estimates on how the surface affects chain conformation.

$r_\tau \ll 1$; *unentangled Rouse dynamics*

The monomeric solution is rapidly polymerized around the attached chain 'switching on' a Gaussian environment; the chain collapses towards a Gaussian conformation via unentangled Rouse dynamics.

Consider polymer A in motion subject to Rouse dynamics; that of connected Brownian beads[9]. The motion of the connected beads, at positions $(\boldsymbol{R}_1, \boldsymbol{R}_2, \ldots, \boldsymbol{R}_N) \equiv \{\boldsymbol{R}_n\}$, is described by the Langevin equation:

$$\zeta \frac{d}{dt}\boldsymbol{R}_n(t) = k\frac{d^2}{dn^2}\boldsymbol{R}_n(t) + f_n(t) \qquad k = \frac{3k_B T}{b^2} \qquad (10)$$

subject to the asymptotic boundary conditions:

$$\langle [\boldsymbol{R}_n(t) - \boldsymbol{R}_m(t)]^2 \rangle = b^2 |n-m|^{2\nu}$$
$$\nu = 3/5 \text{ at } t = 0;\ \nu = 1/2 \text{ as } t \rightarrow \infty \qquad (11)$$

ζ is the friction constant for a bead and $f_n(t)$ is a random force. To get $\langle [\boldsymbol{R}_n(t) - \boldsymbol{R}_m(t)]^2 \rangle$ in the form $F(t, |n-m|)$ we introduce (independent) normal coordinates $\boldsymbol{X}_p$, such that:

$$\boldsymbol{R}_n(t) = 2\sum_{p=1}^{\infty} \boldsymbol{X}_p(t)\sin\left(\frac{(p-1/2)\pi n}{N_A}\right) \qquad p = 1, 2, 3, \ldots \qquad (12)$$

The unusual choice of normal modes is due to the constraint of the fixed, tethered chain end. This gives:

$$\langle [\boldsymbol{R}_n(t) - \boldsymbol{R}_m(t)]^2 \rangle = 4\sum_{p=1}^{\infty}\left[1 - \cos\left(\frac{p\pi|n-m|}{N_A}\right)\right]\langle [\boldsymbol{X}_p(t)]^2 \rangle \qquad (13)$$

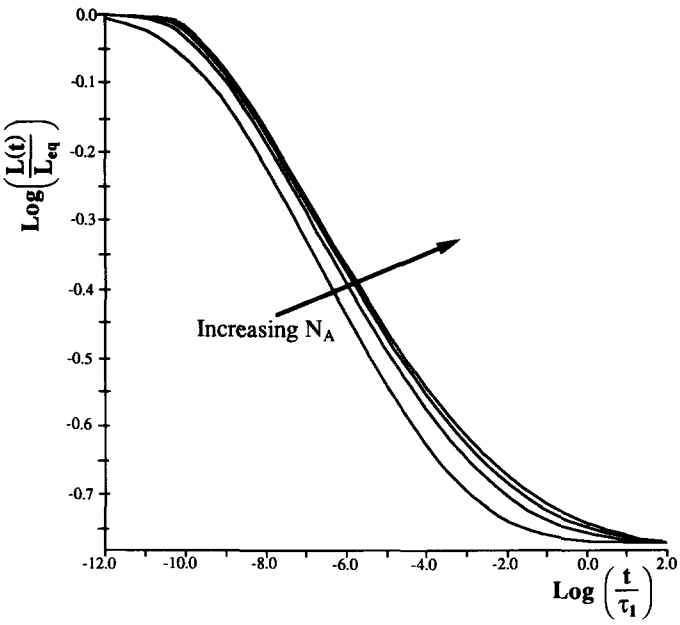

Figure 2 The tube length at the quench time, for the case of a chain relaxing via unentangled Rouse dynamics, and rapid polymerization; $N_A = 3, 6, 10, 15 (\times 10^3)$ from bottom to top; $a = 10$

solving the Langevin equation in $\langle [X_p(t)]^2 \rangle$ gives:

$$\langle [X_p(t)]^2 \rangle = \frac{N_A b^2}{2\pi^2}\left[\left(\frac{N^{1/5}}{p^{11/5}} - \frac{1}{p^2}\right)\exp\left(\frac{-2t}{\tau_p}\right) + \frac{1}{p^2}\right]$$

$$\tau_p = \frac{4\zeta b^2}{3\pi^2 k_B T}\left(\frac{N_A}{p}\right)^2 \qquad (14)$$

where τ_p is the Rouse relaxation time, for the pth mode of the attached chain. The resulting expression for $\langle [\boldsymbol{R}_n(t) - \boldsymbol{R}_m(t)]^2 \rangle$ in the limit of large N_A may be approximated for qualitative purposes by replacing the trigonometric function in equation (12) by a quartic with matched turning points, and the exponential by a step function. The result indicates how the familiar Rouse $t^{-1/2}$ relaxation is modified by the initially swollen statistics:

$$\langle [\boldsymbol{R}_n(t) - \boldsymbol{R}_m(t)]^2 \rangle \approx \frac{4b^2}{\pi^2}\frac{S^2}{N_A} T^{-2/5}\left(\tfrac{10}{9} N_A^{1/5} - T^{-1/10}\right) \times \left(4 - 2\frac{S}{N_A} T^{-1/2} + \frac{S^2}{3N_A} T^{-1}\right) + b^2 S \qquad (15)$$

$$T > (S/2N_A)^2 \qquad T \equiv 2t/\tau_1 \qquad S \equiv |n-m|$$

At $t = t_q$, $|n-m|$ is replaced with N_e and $\langle [\boldsymbol{R}_n(t_q) - \boldsymbol{R}_m(t_q)]^2 \rangle$ is equated to a^2. The solution for $N_e = F^{-1}(a^2, t)$ has to be performed numerically. We know the boundary conditions on $N_e(t)$ from equation (11) and can use them to find the maximum tube length enhancement factor given by:

$$N_e(\infty)/N_e(0) = (a/b)^{1/3} \qquad (16)$$

remembering that the pull-out energy can be proportional to the tube length. *Figure 2* illustrates the solution; the relative relaxation of L is (log–log) plotted against time for several values of N_A. It is clear from the graph that, with increasing N_A, the relaxation time becomes constant. This corresponds to high mode domination of the relaxation process. As one might expect, chain conformations that differ only on length scales much larger than the tube diameter do not differ greatly in their adhesive contributions. Of interest is how the tube diameter a affects the characteristic relaxation time, τ_a. We define this relaxation time arbitrarily by:

$$N_e(\tau_a) = \phi N_e(0) + (1-\phi) N_e(\infty) \qquad \phi = e^{-1} \qquad (17)$$

and plot τ_a against a in *Figure 3*, using the full numerical solution. The power law $\tau_a \sim a^\gamma$ with $\gamma = 3.33$ that is observed is what one would expect for Rouse relaxation ($\tau \sim N^2$), dominated by the swollen conformation. If a becomes comparable to the tube length then the relaxation time becomes that of the whole chain and $\tau \to \tau \approx a^0$. The cross-over between the two power laws is seen as the curvature in *Figure 3*. Although the partially analytic solution gives a good approximation to the tube length relaxation, we found that the approximations were very sensitive to the inversion of equation (15) and gave the result $\gamma = 4.66$, which appears to have no physical origin.

$r_\tau \ll 1$; entangled Rouse dynamics

When the tethered chains undergo most of their relaxation in a bath of long polymers, entanglements will dominate the relaxation itself. Contraction is dominated by the relaxation of the contour length, along the curvilinear axis of the tube, by entangled Rouse dynamics (*Figure 4a*). Only at much later times does contour length

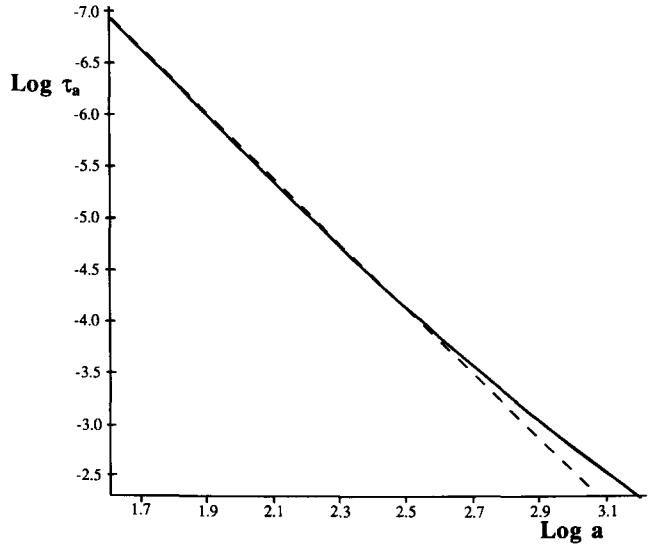

Figure 3 The dependence of the characteristic relaxation time τ_a on the tube diameter a (appearing at the quench), for the case of unentangled Rouse dynamics and rapid polymerization

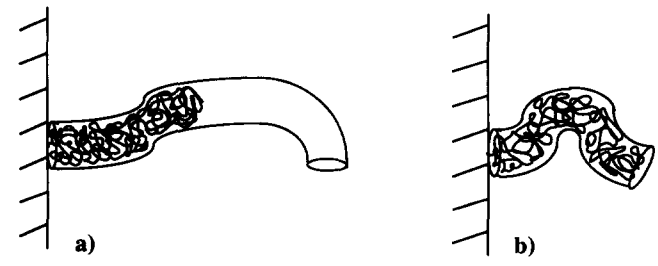

Figure 4 (a) The contour length of the chain relaxes towards its Gaussian equilibrium via tube Rouse dynamics; however, the tube itself remains swollen. (b) Over a timescale $t \sim \exp[N_A/N_e(\infty)]$ the conformation of the tube becomes Gaussian via contour length fluctuation, however, this does not affect the tube length

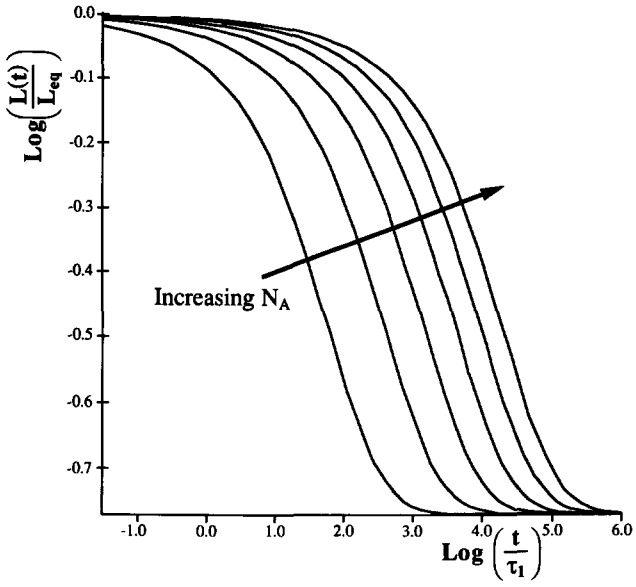

Figure 5 The extent of tube length relaxation, via tube Rouse dynamics, at the quench time for the case of rapid polymerization; $N_A = 10, 15, 20, 25, 30, 35 (\times 10^3)$ from bottom to top; $a = 10$

fluctuation[9] become effective (*Figure 4b*). In fact, this only serves to relax the *tube's* conformation; thus $\langle L(t) \rangle$ and hence E_p will be unaffected. The contour length of the chain is given by:

$$L(t) = S_N(t) - S_0(t) \tag{18}$$

where in the normal coordinate notation:

$$S_n = 2 \sum_{p=1}^{\infty} Y_p \sin\left(\frac{\pi(p-1/2)}{N_A}\right) + \frac{nL_{eq}}{N_A} \tag{19}$$

is the position of the Rouse segment n along the curvilinear axis, where L_{eq} is the equilibrium contour length. Solving the Langevin equation for $\langle Y_p(t) \rangle$ gives:

$$\langle L(t) \rangle = L_{eq} + \frac{12}{\pi^2}[\langle L(0) \rangle - L_{eq}] \sum_{p=1}^{\infty} \frac{(-1)^p}{p^2} \exp\left(\frac{-p^2 t}{\tau_1}\right) \tag{20}$$

$$\langle L(t) \rangle = (a^{\nu-1}b)^{1/\nu} N_A \qquad \nu = 3/5 \text{ at } t = 0;\ \nu = 1/2 \text{ as } t \to \infty$$

In this case $\langle L(t) \rangle$ is dominated by the first mode ($\sim 80\%$) and thus has a much longer relaxation time than in the unentangled Rouse relaxation case. Again the tube length enhancement factor is $(a/b)^{1/3}$. A graph of $\langle L(t) \rangle$ is plotted in *Figure 5* and illustrates the long relaxation time τ, which in this case is not a function of tube diameter a, but of N_A, $\tau \approx (N_A)^2$.

General polymerization/relaxation

We consider here the conformational relaxation of polymer A most generally; the ratio of Rouse relaxation/polymerization time may be comparable, and relaxation starts before polymerization terminates.

During polymerization polymer A experiences three distinct concentrations of solvent polymer; that of dilute, semidilute and concentrated solutions. The average concentration of solvent polymer, throughout polymerization, is given by:

$$C(t)/C(\infty) = N_s(t)/N_s(\infty) \tag{21}$$

where $N_s(\infty)$ and $C(\infty)$ are respectively the values of solvent degree of polymerization and solution concentration at full polymerization. The cross-over from dilute to semidilute solutions signifies the point at which the growing, swollen solvent polymers start to overlap. Thus at the overlap concentration C^*, the local and average concentrations are equal, and given by:

$$C^* = N_s(t)/R_s^3(t) \qquad R_s(t) = bN_s^{3/5}(t) \tag{22}$$

where $R_s(t)$ is the swollen coil diameter of the solvent polymer. The cross-over concentration C^{**}, when going from semidilute to concentrated solutions, occurs when, for the solvent polymers, the ratio of chain intermolecular/intramolecular interactions becomes greater than unity. It is calculated that, in the case of excluded-volume interaction only, $C^{**} \approx 1/\pi$ (ref. 9). As this is of order one and as, for reasonably large values of $N_s(\infty)$, C^* is small, then for simplicity we consider it a good approximation to treat the conformational relaxation in the semidilute regime only.

This semidilute binary solution is characterized by three length scales. First, in a good solvent a chain predominantly interacts only with itself up to the scale of the screening length $\xi(t)$ (ref. 10), such that:

$$\xi(t) \approx b[C(t)/C(\infty)]^{-3/4} \tag{23}$$

The chain segment within the volume $\xi^3(t)$ is swollen and contains g monomers, such that:

$$g(t) = [\xi(t)/b]^{5/3} \tag{24}$$

Secondly, we consider on which scales the solvent polymers act as a good solvent for polymer A. Using the concept that both polymer species are random walks of step length $\xi(t)$, then the solvent polymers are a good solvent for chain segments containing more than n monomers, providing that[10]:

$$n(t)/g(t) > [N_s(t)/g(t)]^2 \tag{25}$$

Above length scales corresponding to this chain length, the attached chain will be swollen, even though they are screened at shorter length scales.

Thirdly, for a good semidilute solution, the tube diameter $a(t)$ is[13,14]:

$$a(t) \approx [C(t)/C(\infty)]^{-3/4} \tag{26}$$

where we choose the prefactor to be $a(\infty)$, the tube diameter in the melt (i.e. full polymerization). The entanglement number is calculated by considering a random walk of step length $\xi(t)$ encompassing a volume $[a(t)]^3$ (ref. 13) and is:

$$N_e(t) = g(t)[a(t)/\xi(t)]^2 \tag{27}$$

However, the discussion so far has centred on the equilibrium semidilute solution, and we know our solution is non-equilibrium. This means that, although a length scale may be screened, it has not necessarily relaxed to its equilibrium conformation, and thus $N_e(t)$ may be somewhat less than the value given in equation (27). More accurately, the entanglement number should be calculated self-consistently using equation (13) (summing over relaxing mode amplitudes), but this is beyond the scope of our calculation.

It is also noted here that in this semidilute solution, the *attached* chain only becomes well entangled when $N_s(t)$ is greater than both $\alpha N_e(t)$ and $[N_A N_e^2(t)]^{1/3}$. In this work we proceed with the simple analysis whereby

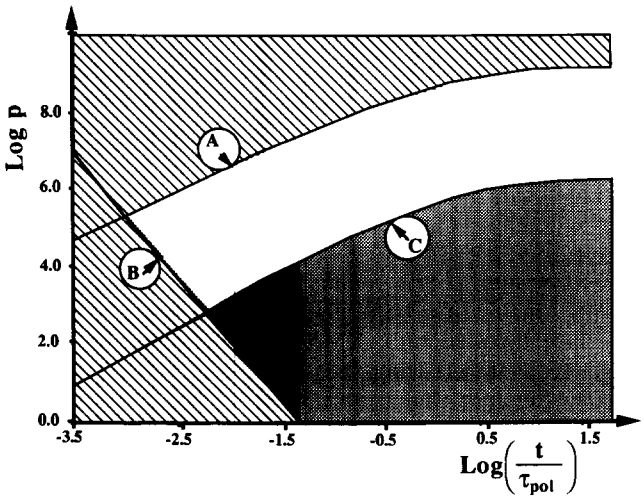

Figure 6 This is the 'relaxation map' for polymer A, with parameter values $N_A = 10^4$, $N_s(\infty) = 10^3$, $a = 5$. The curves are defined by (A) the screening length, (B) the solvent polymer size and (C) the tube diameter. At a given time, modes that reside in the hatched region have not started to relax, those in the white region are relaxing by unentangled Rouse dynamics, those in the grey region are relaxing by entangled Rouse dynamics, and those in the black region, to our approximation of first mode domination, have temporarily stopped relaxing (i.e. they are inside the tube but the first mode is yet to relax)

equations (26) and (27) are valid from the concentration at which the solvent polymers overlap.

To translate an arbitrary segment of m monomers into the corresponding mode of polymer A we use the relationship

$$p_m = N_A/m \tag{28}$$

Substituting equations (24) and (25) into (28) we find that the modes of polymer A that are able to relax are given by the inequality:

$$\frac{N_A}{N_s^2(\infty)}\left(\frac{N_s(t)}{N_s(\infty)}\right)^{-13/4} < p < N_A\left(\frac{N_s(t)}{N_s(\infty)}\right)^{5/4} \tag{29}$$

These are the modes that correspond to the length scales just screened by the growing solvent chains at time t. As a consequence, modes not only have different relaxation times, but also different relaxation starting times. The relaxation starting time, t_p, of a mode p is given by rearranging equation (29) and substituting into the small-time approximation of equation (6), $\tau_{pol}(t)/\tau_{pol}(\infty) \approx N_s(t)/N_s(\infty)$. This is valid in the first instance for the relaxation of significant modes, and secondly for reasonable high values of $N_s(\infty)$:

$$t_p \approx \begin{cases} (p/N_A)^{4/5}\tau_{pol} & p > N_A/N_s^{5/9}(\infty) \\ [N_A/pN_s^2(\infty)]^{4/13}\tau_{pol} & p < N_A/N_s^{5/9}(\infty) \end{cases} \tag{30}$$

The stated inequality in equation (30) dictates by which process (small- or large-scale screening) a mode is motivated to relax, and is given by the intersection of the two inequalities in equation (29).

The tube affects the modes such that, if a mode number is less than the entanglement mode $p_e = N_A/N_e(t)$, it relaxes by tube Rouse dynamics. Making the approximation that, in the tube, conformational relaxation is brought about solely by the first mode, if a mode satisfies:

$$p < \frac{N_A}{N_e(\infty)}\left(\frac{N_s(t)}{N_s(\infty)}\right)^{5/4} \tag{31}$$

further relaxation is coupled to that of the first mode.

The three inequalities on p are represented pictorially in *Figure 6*. The different regions indicate the state and process of relaxation of a mode p, at a reduced time t/τ_{pol}. The entanglement number $N_e(t)$ may be calculated in a similar way to the first scenario: using our 'relaxation map' a summation over current mode amplitudes $\langle[X_p(t)]^2\rangle$ may be performed. However, if the system is quenched during polymerization, $\langle[R_n(t) - R_m(t)]^2\rangle$ must be equated to $[a(t)]^2$. To complement the relaxation map, the contribution of a particular decade of modes to the relaxation of polymer A on the length scale of the melt tube diameter is illustrated in *Figure 7*. This quantifies our earlier observation that the final entangled path length is dominated by the structure of modes such that $p \sim N_A/N_e$. The solution of $N_e(t)$ is performed numerically, and is illustrated in *Figure 8* by plotting $L(t)/L_{eq}$ against t/τ_{pol} (where L_{eq} is the equilibrium tube length in the melt), for a number of different values of τ_1/τ_{pol}. We note that in the case of $\tau_1/\tau_{pol} \sim 1$, there is negligible conformational relaxation during polymerization, taking us back to the rapid polymerization scenarios. However, polymerization on this timescale may well be impracticable.

THE SURFACE

The surface may affect both the statics and dynamics of the attached chain. Owing to the nature of fixing one end of the chain, the Rouse relaxation time is increased by a factor 4. To our knowledge there has not been a rigorous treatment of a single, swollen, terminally attached polymer at a surface. However, it has been calculated[15,16], for a single chain in Θ conditions, that the surface perturbs such that:

$$\langle R^2\rangle = (\langle R^2\rangle_x^{fs} + \langle R^2\rangle_y^{fs} + 2\langle R^2\rangle_z^{fs})/3 \tag{32}$$

where R is the end-to-end vector, z is the direction normal to the surface and fs denotes free solution. It is useful in

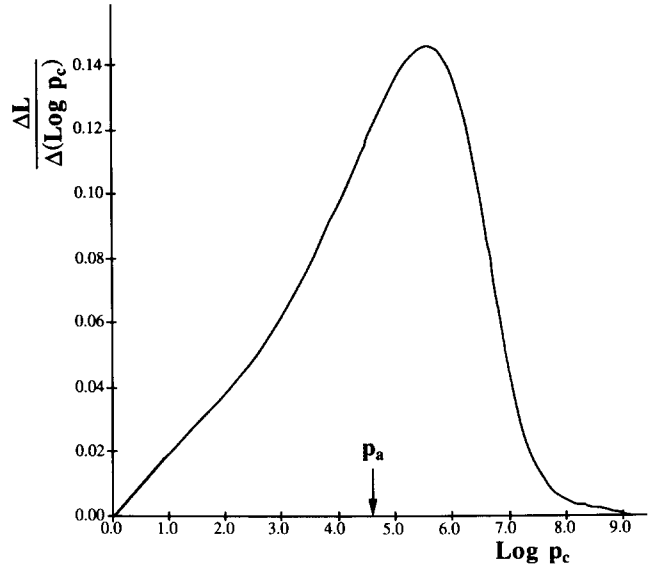

Figure 7 This graph shows the relative contribution, from a particular decade of modes, to the relaxation of the final tube length. The curve was produced by performing a sum over mode amplitudes such that if a mode $p < p_c$ then it had its swollen amplitude, and if $p > p_c$ then the mode had its Gaussian amplitude. The gradient of the resulting graph (L against $\log p_c$) plotted against $\log p_c$ is shown here. The mode corresponding to the tube diameter is indicated

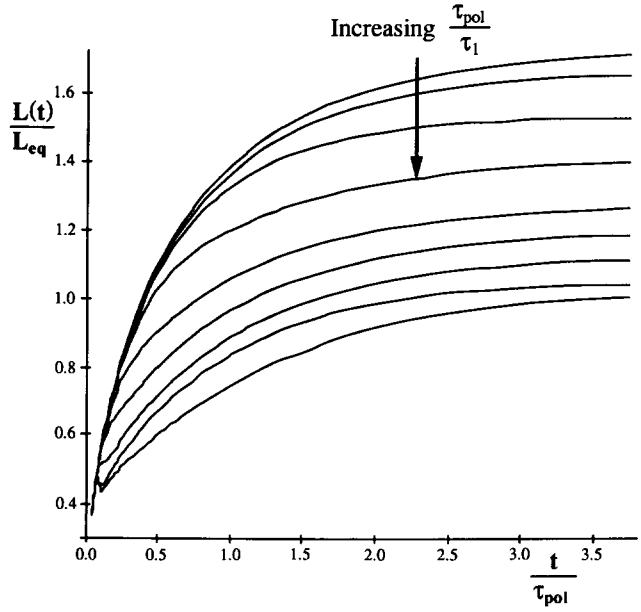

Figure 8 A plot of the current tube length $L(t)$ relative to the tube length at equilibrium in the melt, L_{eq}, during polymerization. The parameter values are $N_A = 10^4$, $N_s(\infty) = 10^3$, $a = 5$; and $\tau_1/\tau_{pol} = 10^{\beta}$ where $\beta = -8$ to 0 for the curves from top to bottom. The parts of the curve above the line $L(t)L_{eq} = 1$ represent tube length (adhesion) enhancement over that of the melt

this analysis to represent a particular mode of polymer A as a blob of m monomers, $m = N_A/p$, so that there are p blobs per mode. We make the conjecture that the magnitude of the surface perturbation upon a mode is proportional to the fractional number of blob surface contacts. For a chain of p blobs the fractional number of surface contacts is $\sim(p/R^3)R^2(1/p) \sim p^{-\nu}$. Thus, for both swollen and Gaussian chains the low modes are perturbed more than the high modes.

For the swollen chain, the number of surface contacts will be a factor $(N_A)^{-1/10}$ less than for the Gaussian polymer of the same N_A, if only the normal component of the end-to-end vector is perturbed. However, owing to the nature of the excluded-volume interaction, the components parallel to the surface will also be affected.

We predict here that the surface affects the lower modes of the initial conformation of the swollen chain. Secondly, in the scenario of unentangled dynamics, the high modes that dominate the relaxation and subsequent conformation of the tube length will suffer only a small perturbation from the surface. Thirdly, in the scenario of entangled dynamics, the initial tube length will be increased as this is low-mode-dependent. Relaxation will be unaffected by the surface, as this will be screened by the tube.

So, for the purposes of adhesion, the effect of the surface is well approximated by our choice of normal modes, without further explicit constraints. This is an unusual situation and for example would not be the case if we were to calculate density properties.

DISCUSSION

Let us now imagine a practical scenario for which we can apply our theory. Consider a diblock copolymer with a small block that bonds to a silica surface and the other block being high-molecular-weight poly(methyl methacrylate) (PMMA). A silica plate is placed in a dilute solution of the copolymer ($c < c^*$), which sticks on to the surface like hard spheres. A matrix is then imposed on the surface by either melt welding or polymerizing the solvent. The equilibrium surface coverage of the swollen copolymers, and thus the interface tube coverage, will be, to within a geometric prefactor:

$$\sigma \approx 1/N_A^{6/5} \tag{33}$$

Given that, for PMMA, N_A can be typically $\sim 10^4$ and the monomer length $\sim 10^{-10}$ m, then we can expect $\sigma \sim 10^{15}\,m^{-2}$. In comparison, if we consider a planar interface through bulk PMMA there would be $\sim 10^{18}$ effective chain crossings per square metre[17]. Thus it is clearly the case that the number of chains involved in possible pull-out processes (and thus the energy dissipation) on the silica is very much smaller than in the bulk and thus here we choose to neglect plastic deformation and crazing associated with the bulk.

If we now initiate a crack along the PMMA/silica interface, the total fracture energy G will be to good approximation the van der Waals surface energy γ, plus the unit-area pull-out energy $E_p\sigma$. As the separation of a monomer from the silica surface and the translation of a monomer along a tube both break a van der Waals bond, using scaling arguments, the ratio $E_p\sigma/\gamma \sim N_A^{4/5}$. Thus for large N_A the van der Waals surface energy can be neglected and the surface fracture energy is given by equation (33) and *Table 1*:

$$G \approx E_p\sigma \approx \frac{\zeta v_0 a N_A^{4/5}}{2b^2 N_e} \tag{34}$$

If we consider the two extreme cases of the tethered chain being swollen or Gaussian then:

$$G \approx \frac{\zeta v_0 N_A^{4/5}}{2(b^{\alpha}a^{3-\alpha})^{1/3}} \qquad \alpha_{Gaus} = 0,\ \alpha_{swol} = 1 \tag{35}$$

For bulk PMMA the tube diameter is measured to be ~ 17 monomer lengths[18]. Thus using equation (16) the maximum increase possible in G due to swollen conformations is $\sim(17)^{1/3} \sim 2.5$.

With respect to the practicalities of rapid polymerization, we find by extrapolating PMMA diffusion data (at 390 K)[19] that the Rouse relaxation time of an entanglement segment is $\tau_e \sim 0.1$ s. Thus to see a significant increase in G due to swollen conformations, the timescale of polymerization and subsequent glassification must be of the order $\lesssim 0.1$ s. A possible way to avoid this impracticality might be solvent polymerization below the glass transition of the PMMA, thus suppressing the Rouse dynamics of the attached chain. However, such reactions are often highly exothermic and sustaining a low temperature may be difficult.

To verify the above predictions a silica plate with tethered chains could be prepared with both a melt welded and *in situ* polymerized matrix. A suitable procedure to test the silica/PMMA interface under fracture might be the four-point flexure test[20]. As well as a general increase in G, the sharp transition in G at low N_A (ref. 21), associated with loss of entanglements for the attached chains, would be expected to occur at a lower N_A for the swollen chains.

CONCLUSION

The use of surface-tethered polymers provides a useful way of greatly increasing the fracture energy of a glassy

polymer/solid interface. We provide here a theory for the fracture energy for such an interface when the coverage is low and the attached polymers are well entangled. In the regimes where the whole chain is pulled out of its tube we expect to see an increase in the surface fracture energy if the bulk polymer is rapidly polymerized *in situ*. In the extreme case where the polymerization is completed before any significant motion of the attached chain, the fracture energy will increase by a factor $(a/b)^{1/3}$. This effect could explain anomalies in fracture energies where interfaces have been prepared using different techniques.

With regards to using the effect to strengthen interfaces, careful consideration would have to be given to how long-timescale motion in glassy polymers would affect the 'frozen' non-equilibrium conformation.

It would be useful to have a value for the non-diffusive monomeric friction coefficient ζ for the glassy phase so as to make numerical calculations of the surface fracture energies.

ACKNOWLEDGEMENTS

This work was financially supported by ICI and the Science and Engineering Research Council. We thank R. P. Wool, J. Edwards and R. Buscall for some useful conversations.

REFERENCES

1 Berger, L. and Kramer, E. *Macromolecules* 1987, **20**, 1980
2 de Gennes, P. G. *J. Phys. Fr.* 1989, 2551
3 Wool, R. P. and O'Connor, K. M. *J. Appl. Phys.* 1981, **52**(10), 5953
4 Brown, H. R., Char, K. and Reichert, W. Proc. 8th Int. Conf. on Deformation, Yield and Fracture of Polymers, 1991
5 Wool, R. P. Proc. 8th Int. Conf. on Deformation, Yield and Fracture of Polymers, 1991
6 Adolf, D. and Tirrel, M. *J. Polym. Sci., Polym. Phys. Edn.* 1985, **23**, 413
7 Kramer, E. *J. Adv. Polym. Sci.* 1984, **52/53**, 1
8 Evans, K. E. *J. Polym. Sci., Polym. Phys. Edn.* 1987, **25**, 353
9 Doi, M. and Edwards, S. F. 'The Theory of Polymer Dynamics', Clarendon Press, Oxford, 1986
10 de Gennes, P. G. 'Scaling Concepts in Polymer Physics', Cornell University Press, Ithaca, NY, 1979
11 Graessley, W. W. *Adv. Polym. Sci.* 1974, **16**, 1
12 Doi, M., Graessley, W. W., Helfand, H. and Pearson, D. S. *Macromolecules* 1987, **20**, 1900
13 Colby, H. and Rubinstein, M. Preprint, 1989
14 Kavassalis, T. A. and Noolandi, J. *Macromolecules* 1989, **22**, 2709
15 Fitzgibbon, D. R. and McCullough, R. L. *J. Polym. Sci., Polym. Phys. Edn.* 1989, **27**, 655
16 Dolan, A. K. and Edwards, S. F. *Proc. R. Soc. Lond.* (*A*) 1974, **337**, 509
17 Vincent, P. I. *Polymer* 1972, **13**, 558
18 Prentice, P. *Polymer* 1982, **24**, 345
19 Adolf, D. and Tirrell, M. *J. Polym. Sci., Polym. Phys. Edn.* 1985, **23**, 413
20 Ritter, J. E. and Conley, K. Proc. 8th Int. Conf. on Deformation, Yield and Fracture of Polymers, 1991
21 Kramer, E. J. *J. Mater. Sci.* 1978, **14**, 1381